A simple technique for the dispersion analysis of fabry-perot cavity leaky-wave antennas

Mateo-Segura, C.; García-Vigueras, M.; Gómez-Tornero, J.L.; Goussetis, G.; Feresidis, A.P.

DOI:
10.1109/TAP.2011.2167900

A Simple Technique for the Dispersion Analysis of Fabry-Perot Cavity Leaky-Wave Antennas

Carolina Mateo-Segura, *Student Member, IEEE*, Maria García-Vigueras, *Student Member, IEEE*, George Goussetis, *Member, IEEE*, Alexandros P. Feresidis, *Senior Member, IEEE* and Jose Luis Gómez-Tornero, *Member, IEEE*

***Abstract*— A simple analysis technique to extract the complex dispersion characteristics of thin periodic 2-D Fabry-Pérot leaky wave antennas (LWA) is presented. The analysis is based on a two-stage process that dispenses with the need for root-finding in the complex plane. Firstly, full-wave MoM together with reciprocity is employed for the estimation of the LWA radiation patterns at different frequencies from which the phase constant is calculated. Employing array theory the phase constant is subsequently used to estimate the radiation patterns for different values of the leakage rate. The correct value for the leakage rate is identified by matching the corresponding radiation pattern to that obtained using the full-wave method. To demonstrate this technique, we present results for half-wavelength and sub-wavelength profile LWAs. Unlike the transverse equivalent network method, the proposed technique maintains its accuracy even for antennas with low profile.**

***Index Terms*—leaky-wave antenna (LWA), frequency selective surface (FSS), periodic structures, resonant cavities.**

I. Introduction

High gain antennas consisting of a 2-D periodic metallodielectric array suspended above a ground plane at a distance of approximately half-wavelength have been presented in the past [1] and have recently received increased attention [2-7]. They offer a simple solution for achieving highly directive patterns from a single low-directivity source. To a first approximation, their operation can be modeled by a Fabry-Pérot resonant cavity formed between the periodic array acting as a partially reflective surface (PRS) and the fully reflective ground plane [2]. The resonance condition ensures that the radiation emitted by a point source inside the cavity is converted into a directive beam on the other side of the PRS. Antennas of this type have been also realized using stacks of uniform dielectric layers of different thickness [8-10]. However, periodic metallodielectric PRS, which are compatible with commonly employed printed circuit techniques, minimize the number of required layers and offer increased design flexibility.

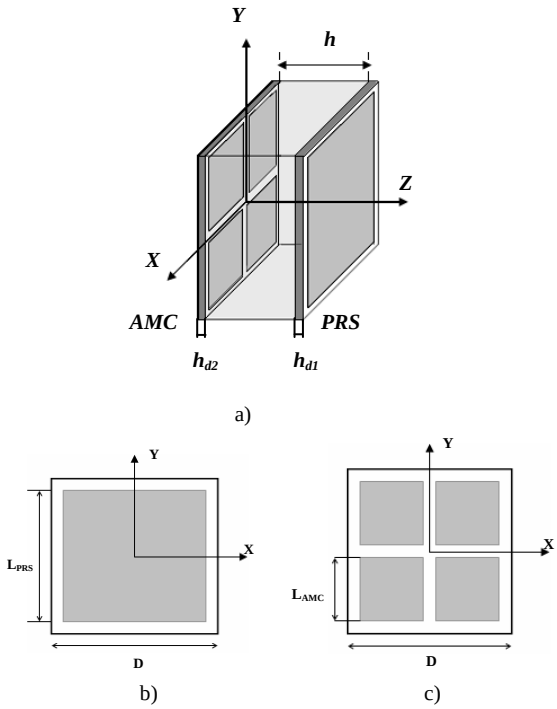

Fig. 1. a) Layout of the resonant cavity leaky-wave antenna formed by metallodielectric PRS and AMC with excitation source inside the cavity b) Unit cell of a square patch PRS array and c) AMC array.

More recently, planar 2-D periodic metallic arrays printed on a grounded dielectric substrate have been presented as artificial magnetic conductors (AMC). Such structures exhibit a high surface impedance for incident plane waves within a specific frequency range [11-14], so that the average tangential magnetic field is small and the electric field large along the surface [15]. Due to this unusual boundary condition, AMC structures reflect incident plane waves in–phase to the incident field and can be used as ground planes for low-profile antennas. Employing this type of ground plane

Manuscript received February 23, 2009. G. Goussetis wishes to acknowledge the support by the Royal Academy of Engineering under a five-year research fellowship.

C. Mateo-Segura and G. Goussetis were with the Institute for Integrated Systems, Heriot-Watt University, Edinburgh EH14 4AS, UK. C. Mateo-Segura is now with the Wireless Communications Research Group, Department of Electronic and Electrical Engineering, Loughborough University, Leicestershire LE11 3TU, UK, (e_mail: c.mateo@ieee.org). G. Goussetis is now with the Institute of Electronics Communications and Information Technology (ECIT), Queen's University Belfast, Northern Ireland, BT3 9DT, UK (G.Goussetis@ieee.org).

A.P. Feresidis is with the Wireless Communications Research Group, Department of Electronic and Electrical Engineering, Loughborough University, Leicestershire LE11 3TU, UK. (e_mail: a.feresidis@lboro.ac.uk).

M. García-Vigueras and J.L. Gómez-Tornero are Departamento de Tecnologías de la Información y las Comunicaciones, Technical University of Cartagena, Antiguo Hospital de Marina, Cartagena 30202, Spain (e-mail: maria.garcia@upct.es; josel.gomez@upct.es).

(Fig. 1), Fabry-Pérot type LWAs with quarter wavelength [16] and sub-wavelength [17] profiles have been reported.

Several techniques have been proposed for the analysis and design of infinite Fabry-Pérot Leaky Wave Antennas (LWAs). An approximate ray-optics model was employed in [1] to extract the radiation pattern and the resonance condition. In [8] a transmission line model was introduced in order to predict the radiation characteristics and resonance conditions of antennas formed using multiple layers of dielectrics. More recently, the radiation patterns of Fabry-Pérot antennas formed by 2-D periodic metallodielectric arrays as PRS have been extracted using rigorous full-wave Method of Moments (MoM) and invoking reciprocity [4,18]; however, this technique stops short of obtaining the complex propagation constant, which is useful for the design of antennas with tailored radiation patterns.

The radiation characteristics of infinite LWAs can also be obtained by the complex wavenumber of the associated leaky mode [7, 9]. The wavenumber dispersion allows estimation of the antenna radiating aperture profile, which in turn can be used to obtain the far-field radiation patterns, their beamwidths and associated bandwidths, as well as the variation of the antenna pointing angle with frequency [19]. Knowledge of the complex dispersion relation is also helpful in the synthesis of practical LWAs. For example, the leakage rate allows estimation of the power radiated within a finite antenna length, which is essential in designing finite LWAs with high radiation efficiency. The complex wavenumber is also required for the systematic design of a non-uniform LWA, which can produce tapered illumination patterns that avoid phase aberration [19-21], leading to far-field patterns with reduced side-lobes and antenna systems prone to reduce interference.

The complex dispersion of Fabry-Pérot LWAs with a PRS consisting of 2-D periodic metallodielectric arrays was first extracted in [22] employing a Transverse Equivalent Network (TEN) and a pole-zero method to estimate the equivalent impedance of the array. Since a single mode TEN is employed, the accuracy of this technique is reduced for sub-wavelength profile antennas. Although it is possible to produce multiport TEN [23] and other formulations of the eigenvalue problem to obtain the complex dispersion of bound and leaky modes of 2D periodic structures using full-wave techniques, such as MoM [22], the associated eigenvalue equations, zeros of the impedance matrix equation, typically take non-canonical form [24-25], which is cumbersome to solve numerically in the complex plane. Techniques based on the Finite-Difference Time-Domain (FDTD) method have also been developed in order to extract the dispersion of the complex wavenumber for this type of antennas [26-27]. These techniques can be time consuming and, particularly for very small or large values of the leakage rate, have limited accuracy.

In this paper, we propose a new simple technique for the estimation of the complex dispersion of thin periodic 2-D LWAs in the leaky wave region. The technique combines for the first time array theory as well as periodic MoM with reciprocity. An overview of the method is given in section II. Subsequently, the technique is applied in section III in order to study three different antenna designs, namely a half-wavelength, a quarter-wavelength and a sub-wavelength ($\lambda/7$) profile 2-D LWAs. The radiation patterns and the complex dispersion are derived employing the proposed method and compared with those obtained using a TEN.

II. Dispersion of Fabry-Perot Leaky-Wave Antennas

The complex wavenumber, $\boldsymbol{k}$, of a leaky-mode in general takes the form:

$$\boldsymbol{k} = \beta - j\alpha \quad (m^{-1}) \tag{1}$$

where β is the phase constant and α is the leakage rate. The complex nature of $\boldsymbol{k}$ expresses the decrease of the amplitude of the leaky wave as it propagates due to radiation. In the absence of other sources of radiation, the phase constant, β, determines the pointing angle, θ, of the antenna's main lobe and the leakage rate, α, determines the illumination of the radiating aperture. Significantly, the radiation pattern of a LWA can be obtained analytically for a uniform LWA with a given complex wavenumber [19, 28]. The method that we propose here is based on the following procedure; the radiation pattern of a particular infinite-size LWA is initially obtained using full-wave periodic MoM and invoking reciprocity [4]. Subsequently an iterative procedure is employed based on array theory [28-29] in order to reproduce this pattern from pairs of β and α. Since the calculations involved in this iterative process are analytical, and since prior knowledge of the propagation constant, β, can be obtained by the angle of maximum radiation, the proposed technique is fast and computationally efficient. In the following we present the method and the analytical expressions involved in the calculation of the radiation patterns.

A. Spectral Domain Periodic MoM and Reciprocity

Reciprocity suggests that the far-field radiated at a certain direction by an antenna fed by a point source is proportional to the relative excitation of the near fields at an observation point upon plane wave incidence from the same direction. Hence, by scanning the relative field strength at an observation point inside the antenna cavity for plane waves incident with all possible angles at a fixed frequency, the radiation pattern of the antenna at this frequency can be obtained [4, 18]. This method can be efficiently applied employing the spectral domain periodic MoM for the full-wave modeling of LWAs such as the one depicted in Fig. 1. The Electric Field Integral Equation (EFIE) is determined by applying the boundary condition on the metallic elements that compose the array (here assumed perfect conductors), and subsequently solved using the Galerkin MoM. For simple array element geometries, such as the one shown in Fig. 1, the currents can be modelled using zero-ended entire domain sinusoidal basis functions [30, 31], yielding fast and accurate results. The details of this method are described elsewhere and therefore not repeated here [4, 30].

B. Array factor approach

The array factor (AF) approach serves as an alternative method to calculate the radiation characteristics of periodic

LWAs [28, 29]. The array factor for a 2-D planar array is given by the following expression [29]:

$$AF(\theta,\varphi)=\left[\sum_{m=-\frac{M}{2}}^{m=\frac{M}{2}} I_{m1}e^{j(m-1)(k_0 D_x \sin\theta\cos\varphi)+j\xi_m}\right]\cdot \left[\sum_{n=-\frac{N}{2}}^{n=\frac{N}{2}} I_{1n}e^{j(n-1)(k_0 D_y \sin\theta\sin\varphi)+j\xi_n}\right] \quad (2)$$

where D_x / D_y is the periodicity and M / N is the number of unit cells along the x- / y- axis respectively. For an infinitely long antenna there is no contribution to the radiation by edge effects. The phase ξ_m /ξ_n in Eq. 2 represents the relative phase shift of the excitation for the m / n order element referenced to the element at the origin. Assuming that all higher Floquet space harmonic (FSHs) are evanescent and only the fundamental can radiate, then the relative phase shift is determined by the propagation constant, $\beta_{x/y}$, of the fundamental FSH in the x- / y- directions:

$$\xi_m=-(m-1)\beta_x D_x \qquad \xi_n=-(n-1)\beta_y D_y \quad (3)$$

The relevant excitation strength of the m^{th} / n^{th} array element, I_{m1}/I_{1n} in Eq. 2, can be obtained from the attenuation rate, α_x / α_y, due to the leakage, as well as the magnitude of the reference element, I_o. Since for a uniformly periodic array the leakage rate, α, is constant along the antenna, the excitation strength drops exponentially for elements away from the excitation point. To a step approximation, we can therefore write for the m^{th} / n^{th} element along the x- / y-axis:

$$I_{m1}=I_0 e^{-\alpha_x(m-1)D_x} \qquad I_{1n}=I_0 e^{-\alpha_y(n-1)D_y} \quad (4)$$

The radiation pattern of the antenna under consideration can be obtained as the product of the array factor with the radiation pattern of the PRS array element. In this example we assume a free-standing PRS consisting of square patches with edge L (Fig. 1) whose radiation intensity, U , at every (θ,φ) can be obtained using Babinet's principle from that of a rectangular aperture [29]:

$$U(\theta,\varphi)=\frac{\pi^2\eta_0(L\cdot L)^2|E_o|^2}{8\lambda_0{}^2}\left[\frac{\cos\left(\frac{k_0 L}{2}\sin\theta\cos\varphi\right)}{\left(\frac{k_0 L}{2}\sin\theta\cos\varphi\right)^2-\left(\frac{\pi}{2}\right)^2}\right]^2 \cdot\left[\frac{\sin\left(\frac{k_0 L}{2}\sin\theta\sin\varphi\right)}{\frac{k_0 L}{2}\sin\theta\sin\varphi}\right]^2\cdot\left(\sin^2\varphi+\cos^2\theta\cos^2\varphi\right) \quad (5)$$

where k_0 is the free space wavenumber, η_0 is the intrinsic impedance and E_o is a constant. By combining Eq. 2 and 5, the radiation pattern of a LWA such as the one depicted in Fig. 1 can be analytically obtained for a given wavenumber $\boldsymbol{k}$.

C. Derivation of the complex propagation constant

As shown above, the estimation of the radiation pattern following an array factor approach requires prior knowledge of both the real, β, and imaginary, α, part of the wavenumber, $\boldsymbol{k}$. In order to reduce the complexity of the problem, the former can be obtained by tracking the angle of maximum directivity in the full-wave radiation pattern. In particular, in order to extract the dispersion of the propagation constant in a particular direction the radiation pattern of the antenna under consideration is obtained at different frequencies. The angle, θ, corresponding to the direction of maximum directivity for each frequency is then related with β by means of simple trigonometry [19] (Fig. 2):

$$\beta=k_0\cdot\sin\theta \quad (6)$$

where k_0 is the free-space wavenumber. In the following we assume that the antenna of Fig. 1 is excited by a Hertzian dipole polarized along the y-axis. In this case, β_x / β_y correspond to the phase constants along the H- / E-plane and can be obtained by varying the angle of the incident wave along the xz- / yz-planes respectively.

Subsequently, the AF approach is employed to obtain the dispersion of the leakage rate, α. This can be estimated using an inverse and iterative procedure. For each frequency point, we use the corresponding value of the propagation constant, β, and the radiation pattern is successively estimated according to Eq. 2 for different values of the leakage rate, α. For each value of α, the corresponding radiation pattern is compared with the one derived using full wave MoM [30] and reciprocity [4]. This is done by calculating an error function which is expressed as the mean-square error between the two normalised patterns. The value of α for which the error function is minimized corresponds to the actual value of the leakage rate at the particular frequency. For a new frequency point, estimations of the leakage rate at nearby frequencies can be used as starting values, also considering that higher frequencies typically produce lower leakage rates. Since the calculations involved in the iterative procedure are analytical, the proposed method is fast and efficient.

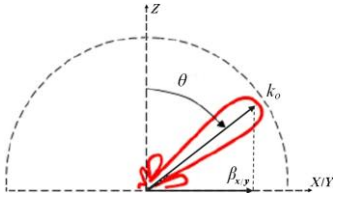

Fig. 2. Estimation of the propagation constant from the angle of maximum gain at the H-plane (β_x) and the E-plane (β_y) for a LWA.

III. Numerical Results

In this section we initially demonstrate the application of the proposed method in working examples of resonant cavity antennas with a single periodic array (PRS) and half-wavelength profile. This refers to the structure shown in Fig. 1 where a Perfect Electric Conductor (PEC) at h=λ/2 is used instead of an AMC. Subsequently, we extend this technique to the case of antennas with two periodic arrays (PRS and AMC)

and sub-wavelength profile; structure shown in Fig. 1 where h is either λ/4 or λ/7. The results from the proposed technique are compared with those from a TEN, where a pole and zero method is employed for the estimation of the effective impedance of the arrays. The latter is very well described in [32, 33] and therefore applied here directly.

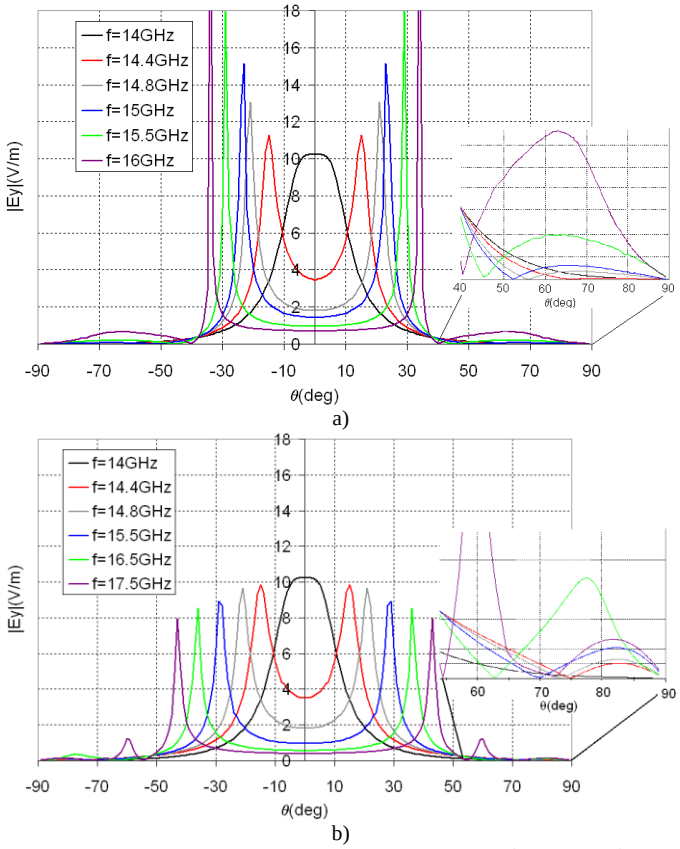

Fig. 3 Radiation pattern a) H-plane and b) E-plane of the LWA formed with a square patch PRS with dimensions (in mm) D= 9.0, L_{PRS}=8, h_{d1}=1.5, h=9.82 and ε_r=2.55.

A. Half-wavelength antennas

The structure under consideration involves a PRS consisting of square patches with edge 8.0 mm arranged in a square lattice with periodicity 9.0 mm and printed on a dielectric slab of thickness, h_{d1}, equal to 1.5 mm and relative permittivity 2.55. This PRS is located at a distance, h, equal to 9.82 mm above a ground plane. This corresponds to approximately half-wavelength at 14GHz, where the antenna produces a broadside pattern. The excitation is assumed to be a Hertzian dipole polarized along y and placed in the middle of the cavity (e.g. z=h/2).

Periodic MoM in the spectral domain is employed to obtain the y-polarised fields at the centre of the unit cell and z=h/2 (observation point). On the calculation of the near fields an optimized number of 40 FSH is considered for convergence better than 1%, [34]. The H- and E- plane radiation patterns for this LWA are obtained by the full-wave method discussed in section IIA for a range of frequencies between 14GHz and 16.5GHz for the H-plane and between 14GHz and 18GHz for the E-plane. Some examples of these results are presented in Fig. 3. Tracking the angle of maximum, θ, and using equation 6, the dispersion of the phase constant is readily obtained.

In agreement with previous studies of 2-D LWA Fig. 3 shows that at broadside a pencil beam is produced with equal 3dB beamwidth in the H- and E-plane [35]. The patterns in the E- and H-plane are increasingly different at higher angles towards endfire. Further observation of this figure shows that as the beam angle increases, the peak field amplitude increases in the H-plane. The opposite is happening in the E-plane. These observations are in agreement with [35]. Furthermore, the inset in Fig. 3 shows the presence of grating lobes that correspond to the -1 FSH from 14.4GHz onwards in the H- and the E-plane.

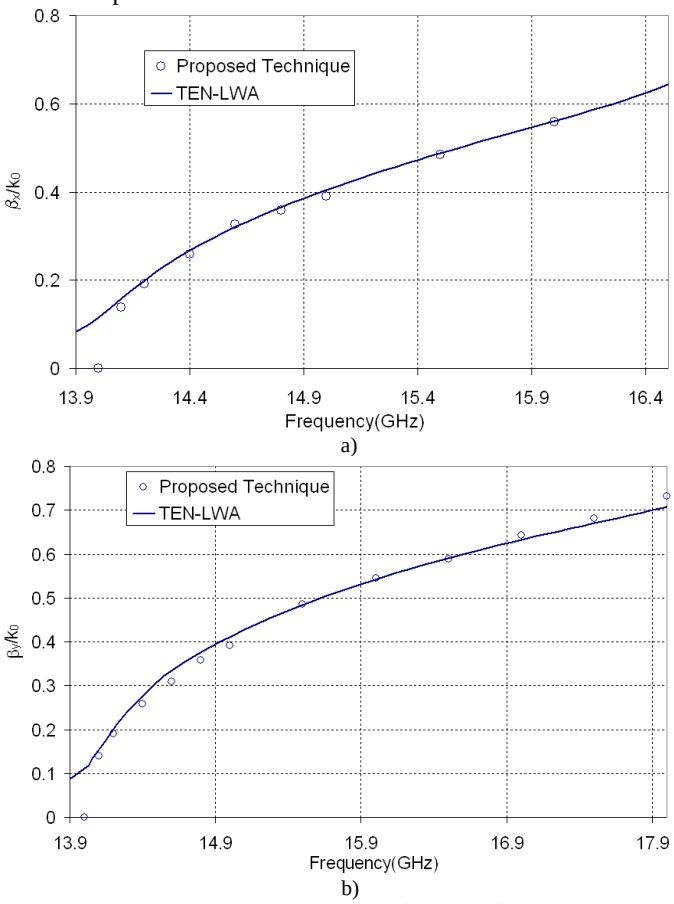

Fig. 4. Normalized wavenumber versus frequency for a) the TE mode along x (H-plane) and b) the TM mode along y (E-plane) as obtained by the proposed technique and a Transverse Equivalent Network for the LWA with dimensions as in Fig. 3.

The dispersion diagrams as obtained from the patterns of Fig. 3 in the frequency range studied are shown in Fig. 4. Based on equation (6), the H-plane pattern provides the phase constant β_x of a TE mode along x, and the E-plane pattern gives β_y corresponding to a TM mode along y [32]. This figure also shows superimposed the phase constant values as obtained from a TEN model [33]. A comparison of the values for β_x / β_y indicates a very good agreement between the two techniques.

Figure 5 shows the radiation pattern calculated according to full-wave MoM together with that estimated using the AF approach assuming an infinitely long antenna with the obtained leakage rate, α. Since the AF calculation is based on the assumption of a single radiating Floquet space harmonic, it cannot predict the side lobes that emerge as a result of higher

Floquet space harmonics in Fig. 5b. Therefore, in the calculation of α, the error function will only include the portion of the radiation pattern that is occupied by the main lobe, neglecting the higher values of θ, which correspond to side lobes.

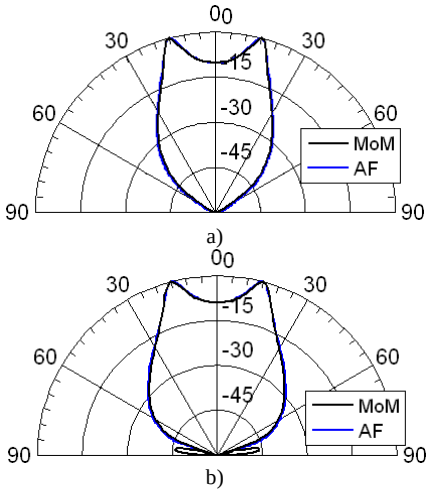

Fig.5. a) H- and b) E-plane radiation pattern at 14.4GHz for the half-wavelength antenna of Fig. 3 as obtained by full-wave Method of Moments and Array Factor theory.

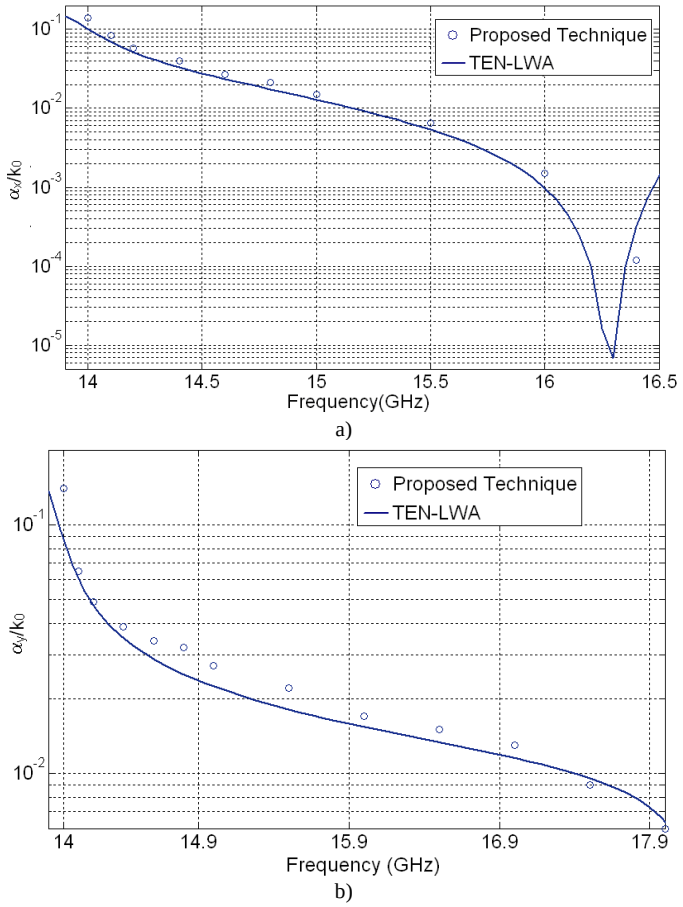

Fig. 6. Normalized leakage rate versus frequency, a) H-plane and b) E-plane as obtained by the proposed technique and a Transverse Equivalent Network for the LWA with dimensions as in Fig. 3.

The computed values of the normalized leakage rate, α, at the H- and E-plane as calculated using the proposed technique as well as the TEN model are shown in Fig. 6. The agreement between both techniques is good for the given range of frequencies. As common with LWAs [19], the normalized leakage rate, α/k_0, decreases towards endfire direction. The interference of the side lobes with the main lobe limits the applicability of the proposed technique at higher frequencies.

B. Quarter wavelength antennas

Antennas with sub-wavelength profile can be produced introducing a second periodic array in close proximity to the ground plane [15, 16]. To a ray optics approximation, this can be attributed to the reduced reflection phase of the AMC ground plane. Here we employ a working example of an antenna such as the one shown in Fig. 1. The PRS employed previously is now located at a distance h= 5.46 mm above an AMC array, which consists of patches with edge, L_{AMC}=4.1 mm and is printed on a dielectric slab of thickness, h_{d2}=1.15 mm and relative permittivity 2.2. The height of the cavity, h, has been designed for the antenna to produce a broadside pattern at 14GHz.

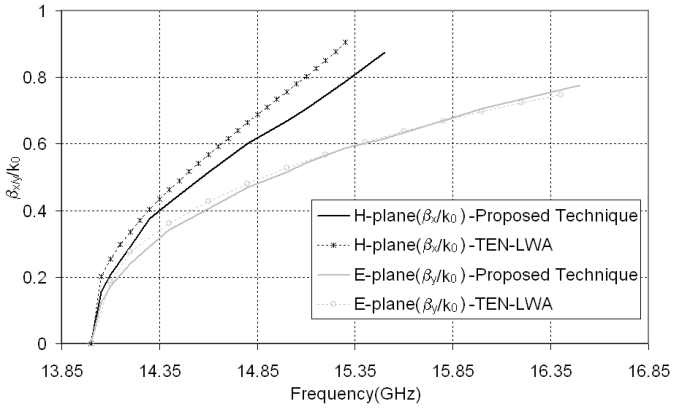

Fig. 7. Normalized wavenumber versus frequency for the H- and E-plane as obtained by the proposed technique and a Transverse Equivalent Network for the sub-wavelength antenna of Fig. 1, with dimensions (in mm) D= 9.0, h=5.46, for the PRS: square patches L_{PRS}=8, h_{d1}=1.5 and ε_r=2.55 and for the AMC: square patches L_{AMC}=4.1, h_{d2}=1.15 and ε_r=2.2 operating at 14GHz.

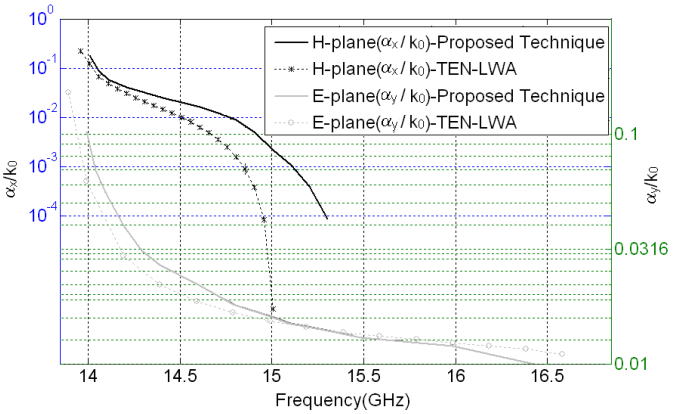

Fig. 8. Normalized leakage rate versus frequency for the H-plane and E-plane as obtained by the proposed technique and a Transverse Equivalent Network for the sub-wavelength antenna of Fig. 7.

A similar study as the one performed for the half-wavelength antenna is carried out. In order to apply the periodic MoM commensurate periodicities are assumed ensuring that the set of FSH is suitable for expanding the fields at both arrays. For

thinner cavities, higher order evanescent FSH can increasingly interact and therefore become increasingly important in the calculation of the near fields and thus in the estimation of the patterns. For this example 60 FSH in the x- and y- direction are considered for a convergence better than 1%, [34].

The dispersion of the phase constants are shown in Fig. 7 for a range of frequencies between 14GHz and 15.6GHz for the H- and between 14GHz and 16.5GHz for the E-plane. This figure also shows superimposed the phase constant values as obtained from a TEN. The computed values of the leakage rate at the H- and E-plane are also depicted in Fig. 8 between 14GHz and 15GHz for the H- and E-plane. The TEN utilised in the calculations only accounts for a single mode, therefore when the antenna profile decreases the accuracy of the method is also reduced. Consequently, as is evident in Figs 7 and 8, the agreement between the two methods for this antenna is reduced compared to the half-wavelength antenna, particularly in the H-plane.

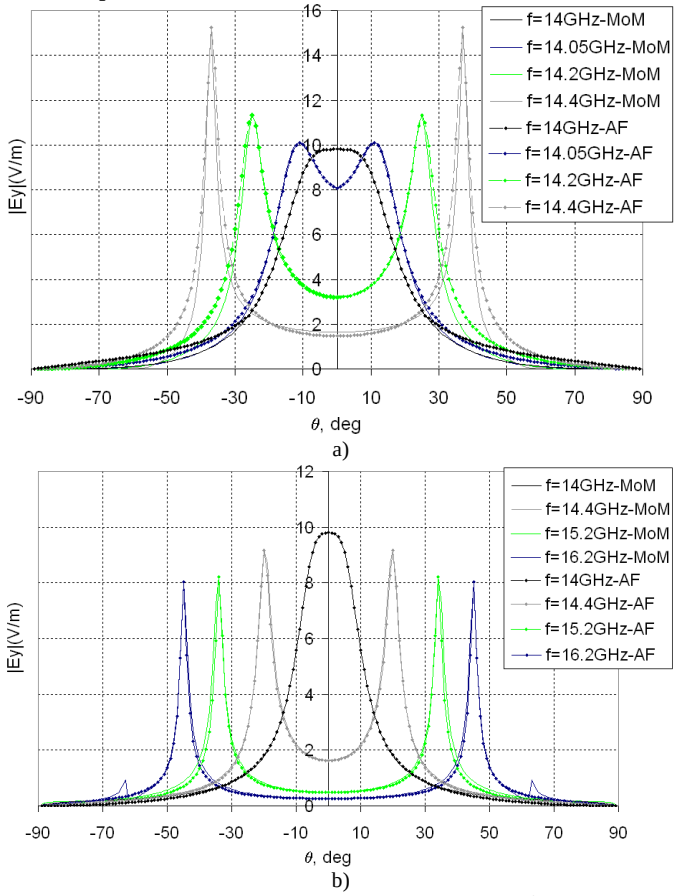

Fig. 9 Radiation pattern a) H-plane and b) E-plane of the LWA with dimensions (in mm) D= 9.0, h=3.25, for the PRS: square patches L_{PRS}=8, h_{d1}=1.5 and ε_r=2.55 and for the AMC: square patches L_{AMC}=4.3, h_{d2}=1.15 and ε_r=2.2 operating at 14GHz as obtained using Full-wave MoM and Array Factor procedure.

C. *Thin antennas*

Thin antennas with sub-wavelength profile can be produced employing an AMC with reflection phase lower than 0^o in the configuration of Fig. 1. Due to the low profile, the interaction of higher order evanescent modes between the two arrays significantly increases. The accuracy of the single mode transverse equivalent network model gradually reduces compared to the half-wavelength profile LWA. The technique proposed here can be directly applied for thin antennas without loss of accuracy. Here we demonstrate this by means of an example involving an antenna with profile λ/7. The PRS is the same as in the previous studies and is located at a distance h= 3.25mm (~λ/7) above an AMC array, which consists of patches with L_{AMC}=4.3 mm printed on a dielectric slab of thickness, h_{d2}=1.15mm and relative permittivity 2.2.

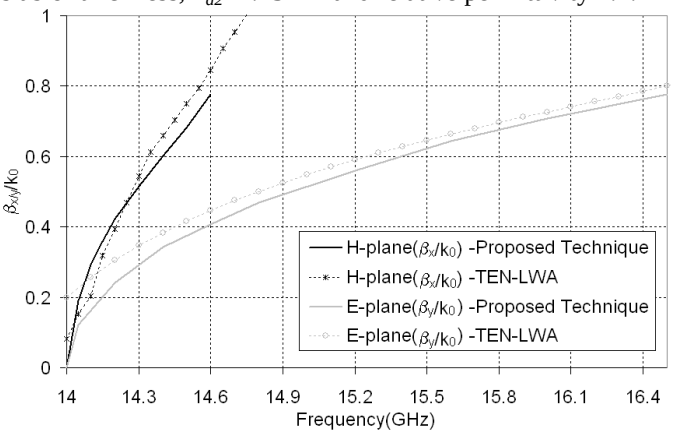

Fig. 10. Normalized wavenumber versus frequency for the H-plane and E-plane as obtained by the proposed technique and a Transverse Equivalent Network for the LWA of Fig. 9.

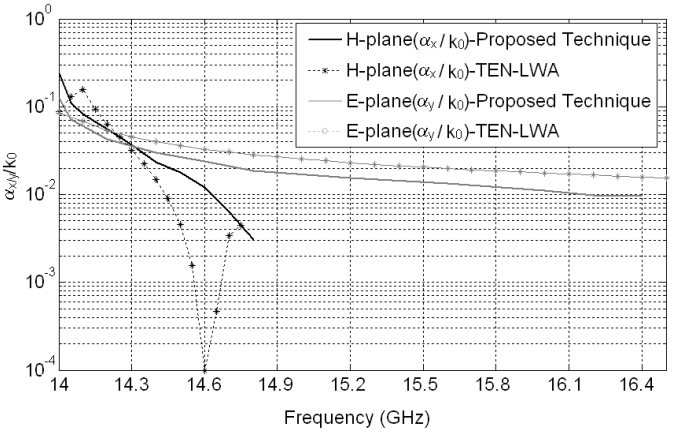

Fig. 11 Normalized leakage rate versus frequency for the H-plane and E-plane as obtained by the proposed technique and a Transverse Equivalent Network for the LWA of Fig. 9.

The H- and E- plane radiation patterns of the LWA at different frequencies are determined in order to extract the phase constant in either plane. A total number of 120 FSH in each direction has been taken into account for convergence better than 1%. The radiation patterns at both planes as obtained using MoM as well as an AF approach at different frequencies are presented in Fig. 9 showing a good agreement between both techniques that validate the AF model accuracy. A pencil beam is obtained at broadside at the frequency of 14GHz. However, a narrower beamwidth is obtained in the E-plane attributed to a lower value of the leakage rate at this plane. The dispersion diagrams for the H- and E-plane are shown in Fig. 10 for frequencies between 14-14.6GHz and 14-16.5GHz, respectively. The interference of the side-lobes with the main lobe impedes the application of the proposed technique in this case beyond 14.6 GHz for the H-plane and

beyond 16.5 GHz for the E-plane. The computed values of the leakage rate are also depicted in Fig. 11 between 14-14.6GHz and 14-15.1GHz for the H- and E-plane, respectively. In both figures, the resulting dispersion parameters as obtained using TEN are depicted clearly showing how the accuracy of the method has reduced even more for the λ/7 antenna, particularly at the H-plane.

IV. Discussion And Conclusion

The antennas under investigation have been designed to operate at 14 GHz using the same PRS but different AMCs, so that the profile of the antenna reduces as the dimension of the lower array (AMC) is increased. By observation of Figures 6, 8 and 11 one can conclude that higher values of the leakage rate are obtained for antennas with reduced profile and the same PRS. This leads to less directive radiation patterns for thinner antennas. For angles away from broadside (frequency higher than 14 GHz) the difference between the values of the leakage rate for antennas with different profiles becomes smaller. Figures 5, 7 and 10 further demonstrate that as the profile reduces, the phase constant $\beta_{x/y}$ varies more rapidly with frequency in both the H- and E- plane. Moreover, the phase constant at the H- (β_x) and E-plane (β_y) take similar values for half-wavelength antenna (Fig. 5a and 5b). However, for thinner antennas the values of the phase constant for angles away from broadside (frequency higher than 14 GHz) increasingly differ being always larger at the H-plane, β_x than at the E-plane, β_y.

In conclusion, a simple technique for the dispersion analysis of high-gain planar leaky-wave antennas employing either one or two periodic surfaces (PRS and AMC) has been presented. MoM together with reciprocity as well as an array factor approach have been used to estimate the complex propagation constant of these antennas. The proposed technique was firstly applied to the analysis of a LWA with half-wavelength profile and subsequently extended to antennas with lower profile. The radiation patterns for the E- and H- plane at different frequencies were obtained using MoM in order to extract the phase constant. The produced dispersion diagrams were in good agreement with those derived by a TEN. Reactive interaction between adjacent layers due to evanescent higher-order Floquet harmonics limits the validity of the single mode TEN, which is based on equivalent impedances of the PRS and AMC arrays and single mode circuits. The proposed technique overcomes this problem, so that low-profile LWAs can be accurately and efficiently analyzed. The main limitation of the proposed technique is due to the appearance of grating lobes, which limit the applicability of the technique.

References

[1] G.V. Trentini, "Partially reflecting sheet arrays", *IRE Trans. Antennas Propag.*, vol. 4, pp. 666-671, 1956.

[2] A. P. Feresidis, and J. C. Vardaxoglou, "High-gain planar antenna using optimized partially reflective surfaces," *IEE Proc. Microw. Antennas Propag.*, vol. 148, No.6, Feb. 2001.

[3] Y. J. Lee, J. Yeo, R. Mittra, and W. S. Park, "Design of a high-directivity electromagnetic band gap (EBG) resonator antenna using a frequency selective surface (FSS) superstrate," *Microwave and Optical Tech. Lett.*, vol. 43, pp. 462–467, Dec. 2004.

[4] T. Zhao, D. R. Jackson, J. T. Williams, Hung-Yu D. Yang, and A. A. Oliner, "2-D Periodic Leaky-Wave Antennas-Part I: Metal Patch Design", *IEEE Trans. Antennas and Propag.*, vol. 53, No. 11, pp. 3515-3524, Nov. 2005.

[5] T. Zhao, D. R. Jackson, J. T. Williams, "2-D periodic leaky-wave Antennas-part II: slot design," *IEEE Trans. Antennas Propag*., vol. 53, no. 11, pp. 3515-24, Nov. 2005.

[6] R. Gardelli, G. Donzelli, M. Albani, and F. Capolino, "Design of Patch Antennas and Thinned Array of Patches in a Fabry-Perot Cavity Covered by a Partially Reflective Surface," in *European Conference on Antennas and Propag*. (EuCAP), Nice, France, 6-10 Nov. 2006.

[7] P. Kosmas, A. P. Feresidis, and G. Goussetis, "Periodic FDTD Analysis of a 2-D Leaky-Wave Planar Antenna Based on Dipole Frequency Selective Surfaces," *IEEE Trans. Antennas Propag.*,vol. 55, No.7, pp. 2006-2012, July 2007.

[8] D.R. Jackson and N.G. Alexopoulos, "Gain Enhancement methods for printed circuit antennas", *IEEE Trans. Antennas and Propag.*, vol. AP-33, No.9, Sept. 1985.

[9] D.R. Jackson, A.A. Oliner and A. Ip, "Leaky-Wave Propagation and Radiation for a Narrow-Beam Multiple-Layer Dielectric Structure", *IEEE Trans. Antennas and Propag.*, vol. 41, No.3, March 1993.

[10] R. Gardelli, M. Albani, F. Capolino, "Array thinning by using antennas in a Fabry-Perot cavity for gain enhancement," *IEEE Trans. Antennas Propag.*, vol. 54, no. 7, pp. 1979-90, Jul. 2006

[11] D. Sievenpiper, Z. Lijun, R.F. Broas, N.G. Alexopoulos and E. Yablonovitch,"High-impedance electromagnetic surfaces with a forbidden frequency band," *IEEE Trans. Microwave Theory and Techniques*, vol. 47, No.11, pp. 2059-2074, Nov. 1999.

[12] G. Goussetis, A.P. Feresidis, J.C. Vardaxoglou, "Tailoring the AMC and EBG Characteristics of Periodic Metallic Arrays Printed on Grounded Dielectric Substrate," IEEE Transactions Antennas and Propagation, vol. 54, No. 1, pp. 82-89, January 2006.

[13] O. Luukkonen, C. Simovski, G. Granet, G. Goussetis, D. Lioubtchenko, A. V. Räisänen, and S. A. Tretyakov, "Simple and accurate analytical model of planar grids and high-impedance surfaces comprising metal strips or patches," *IEEE Trans. Antennas Propag.*, Vol. 56, No. 6, pp. 1624-1632, June 2008.

[14] O. Luukkonen, P. Alitalo, C. R. Simovski and S. A. Tretyakov, "Experimental verification of an analytical model for high-impedance surfaces," *Electronics Letters*, vol. 45, no. 14, pp. 720--721, 2009.

[15] G. Goussetis, A.P. Feresidis and R. Cheung, "Quality factor Assessment of Subwavelength Cavities at FIR Frequencies," Journal of Optics A, Vol. 9, pp. s355-s360, August 2007

[16] A. P. Feresidis, G. Goussetis, S. Wang, and J. C. Vardaxoglou, "Artificial Magnetic Conductor Surfaces and Their Application to Low-Profile High- Gain Planar Antennas," *IEEE Trans. Antennas Propag.*, vol. 53, No. 1, pp. 209-215, Jan. 2005.

[17] S. Wang, A.P. Feresidis, G. Goussetis, J.C. Vardaxoglou, "High-Gain Subwavelength Resonant Cavity Antennas Based on Metamaterial Ground Planes," *IEE Proc. Antennas and Propag.*, Vol. 153, No. 1, pp.1-6, Feb. 2006.

[18] C. Mateo-Segura, G. Goussetis, A.P. Feresidis, "Sub-wavelength Profile 2-D Leaky-Wave Antennas with Two Periodic Layers," *IEEE Trans. Antennas and Propag.*, vol. 59, nº 2, pp. 416-424, Feb. 2011

[19] A. Oliner. "Leaky-wave antennas," in Antenna Engineering Handbook, Third Edition, edited by R. C. Johnson, McGraw Hill, 1993.

[20] J. L. Gómez, D. Cañete and A. Álvarez-Melcón, "Printed-Circuit Leaky-Wave Antenna with Pointing and Illumination Flexibility," *IEEE Microwave and Wireless Components Lett.*, vol.15, No.8, pp.536-538, August 2005.

[21] J.L. Gómez, G.Goussetis, A.Feresidis, and A.A.Melcón, "Control of Leaky-Mode Propagation and Radiation Properties in Hybrid Dielectric-Waveguide Printed-Circuit Technology: Experimental Results," *IEEE Trans. Antennas Propag.*, vol.54, No.11, pp.3383-3390, Nov. 2006.

[22] S. Maci, M. Casaletti, M. Caiazzo, and C. Boffa, "Dispersion properties of periodic grounded structures via equivalent network synthesis," *IEEE Antennas Propag. Int. Symp.*, vol. 1, pp. 493 – 496, 22-27 June 2003.

[23] J.L. Gómez-Tornero, G. Goussetis, D. Cañete-Rebenaque, F. Quesada-Pereira, and A. Álvarez-Melcón, "Simple and Accurate Transverse Equivalent Network to Model Radiation from Hybrid Leaky-Wave Antennas with Control of the Polarization," *IEEE Antennas Propag. Society Int. Symp.*, pp.1-4, 5-11 July 2008.

[24] G. Goussetis, A. P. Feresidis, and P. Kosmas, "Efficient Analysis, Design, and Filter Applications of EBG Waveguide with Periodic

Resonant Loads," *IEEE Trans. Microw. Theory and Tech.*, Vol. 54, No. 11, Nov. 2006.

[25] P. Baccarelli, S. Paulotto, and C. Di Nallo, "Full-wave analysis of bound and leaky modes propagating along 2D periodic printed structures with arbitrary metallisation in the unit cell," *IET Microw. Antennas Propag.*, vol. 1, No. 1, pp. 217—225, 2007.

[26] T. Kokkinos, C. D. Sarris, and G. V. Eleftheriades, "Periodic finite-difference time-domain modeling of leaky-wave structures applied to the analysis of negative-refractive-index metamaterial-based leaky-wave antennas," *IEEE Trans. Microw. Theory Tech.*, vol. 54, pp. 1619–1630, Apr. 2006.

[27] J. R. Kelly, T. Kokkinos, and A. P. Feresidis, "Analysis and Design of Sub-wavelength Resonant Cavity Type 2-D Leaky-Wave Antennas", *IEEE Trans. Antennas Propag.*, vol. 56, nº9, pp. 2817-2825, Sept. 2008.

[28] C. Caloz and T. Itoh, "Array factor approach of leaky-wave antennas and application to 1D/2D composite right/left-handed (CRLH) structures," *IEEE Microwave and Wireless Comp. Lett.*, vol.14, No.6, July 2006, pp. 274-276.

[29] C. A. Balanis, "Antenna Theory: Analysis and Design," Second edition, New York: John Wiley & Sons Inc, 1997.

[30] R. Mittra, C.H. Chan, T. Cwik, "Techniques for analyzing frequency selective surfaces-a review," *Proceedings of the IEEE*, Vol. 76, pp.593-615, Dec. 1988.

[31] J.C. Vardaxoglou, Frequency Selective Surfaces Analysis and Design, John Wiley, 1997.

[32] S. Maci, M. Caiazzo, A. Cucini, M. Casaletti, "A Pole-Zero Matching Method for EBG Surfaces Composed of a Dipole FSS Printed on a Grounded Dielectric Slab," *IEEE Trans. Antennas Propag.*, vol. 53, No. 1, Jan. 2005, pp. 70-81.

[33] M. García-Vigueras, J.L. Gómez-Tornero, G. Goussetis, J.S. Gómez-Diaz, and A. Álvarez-Melcón, "A Modified Pole-Zero Technique for the Synthesis of Waveguide Leaky-Wave Antennas Loaded with Dipole-Based FSS", *IEEE Trans. Antennas Propag.*, vol. 58, No. 6, pp. 1971 – 1979, June 2010.

[34] C. Mateo-Segura, G. Goussetis, and A. P. Feresidis, "Resonant Effects and Near Field Enhancement in Perturbed Arrays of Metal Dipoles", *IEEE Trans. Antennas Propag*, vol. 58, No.8, pp. 2523 – 2530, Aug. 2010.

[35] T. Zhao, D. R. Jackson, J. T. Williams, and A. A. Oliner, "General Formulas for 2-D Leaky-Wave Antennas," *IEEE Trans. Antennas and Propag.*, vol. 53, No. 11, pp. 3515-3524, Nov. 2005.